Linking disease associations with regulatory information in the human genome

Marc A. Schaub,[1] Alan P. Boyle,[2] Anshul Kundaje,[1] Serafim Batzoglou,[1,3] and Michael Snyder[2,3,4]

[1]Department of Computer Science, Stanford University, Stanford, California 94305, USA; [2]Department of Genetics, Stanford University School of Medicine, Stanford, California 94305, USA

Genome-wide association studies have been successful in identifying single nucleotide polymorphisms (SNPs) associated with a large number of phenotypes. However, an associated SNP is likely part of a larger region of linkage disequilibrium. This makes it difficult to precisely identify the SNPs that have a biological link with the phenotype. We have systematically investigated the association of multiple types of ENCODE data with disease-associated SNPs and show that there is significant enrichment for functional SNPs among the currently identified associations. This enrichment is strongest when integrating multiple sources of functional information and when highest confidence disease-associated SNPs are used. We propose an approach that integrates multiple types of functional data generated by the ENCODE Consortium to help identify "functional SNPs" that may be associated with the disease phenotype. Our approach generates putative functional annotations for up to 80% of all previously reported associations. We show that for most associations, the functional SNP most strongly supported by experimental evidence is a SNP in linkage disequilibrium with the reported association rather than the reported SNP itself. Our results show that the experimental data sets generated by the ENCODE Consortium can be successfully used to suggest functional hypotheses for variants associated with diseases and other phenotypes.

[Supplemental material is available for this article.]

Genome-wide association studies (GWAS) have led to the identification of thousands of single nucleotide polymorphisms (SNPs) associated with a large number of phenotypes (Hindorff et al. 2009; Manolio 2010). These studies use genotyping platforms that measure on the order of 1 million SNPs to detect loci that have statistically significant differences in genotype frequencies between individuals who have a phenotype of interest and the general population. Although GWAS provide a list of SNPs that are statistically associated with a phenotype of interest, they do not offer any direct evidence about the biological processes that link the associated variant to the phenotype. A major challenge in the interpretation of GWAS results comes from the fact that most detected associations point to larger regions of correlated variants. SNPs that are located in close proximity in the genome tend to be in linkage disequilibrium (LD) with each other (The International HapMap Consortium 2005, 2007), and only a few SNPs per linkage disequilibrium region are measured on a given genotyping platform. Regions of strong linkage disequilibrium can be large, and SNPs associated with a phenotype have been found to be in perfect linkage disequilibrium with SNPs several hundred kilobases away. Although sequencing can be used to assess associated regions more precisely (Sanna et al. 2011), using sequence information alone is insufficient to distinguish among SNPs that are in perfect linkage disequilibrium with each other in the studied population, and thus equally associated with the phenotype.

Various approaches have been developed to identify variants that are likely to play an important biological role. Most of these approaches focus on the interpretation of coding or other SNPs in transcribed regions (Ng and Henikoff 2003; Adzhubei et al. 2010; Saccone et al. 2010). The vast majority of associated SNPs identified in GWAS, however, are in nontranscribed regions, and it is likely that the underlying mechanism linking them to the phenotype is regulatory. SNPs that influence gene expression (expression quantitative trait loci, eQTLs) (Stranger et al. 2007; Schadt et al. 2008) have been shown to be significantly enriched for GWAS associations (Nicolae et al. 2010; Zhong et al. 2010). Although eQTLs can be used to identify the downstream targets that are likely to be affected by associations identified in a GWAS, they are still based on genotyping methods and therefore also point to regions of linkage disequilibrium rather than to individual SNPs. Methods for identifying SNPs that overlap regulatory elements, such as transcription factor binding sites, are therefore necessary. Approaches based on known transcription factor binding motifs (Xu and Taylor 2009; Macintyre et al. 2010) have been successfully used to refine GWAS results and identify specific loci that have a functional role (Jarinova et al. 2009; Landers et al. 2009). However, the presence of a motif does not imply that a transcription factor is necessarily binding in vivo.

High-throughput functional assays such as chromatin immunoprecipitation assays followed by sequencing (ChIP-seq) (Johnson et al. 2007; Robertson et al. 2007) and DNase I–hypersensitive site (Gross and Garrard 1988) identification by sequencing (DNase-seq) (Crawford et al. 2006; Boyle et al. 2008) can experimentally detect functional regions such as transcription factor binding sites. Experimental evidence shows that the presence of SNPs in these regions leads to differences in transcription factor binding between individuals (Kasowski et al. 2010). A SNP that overlaps an experimentally detected transcription factor binding site and is in strong linkage disequilibrium with a SNP associated with a phenotype is thus more likely to play a biological role than other SNPs in the associated region for which there is no evidence

[3]These authors contributed equally to this work.
[4]Corresponding author
E-mail mpsnyder@stanford.edu

of overlap with any functional data. Several recent analyses of associated regions use these types of functional data in order to identify functional loci in individual diseases (Lou et al. 2009; Carvajal-Carmona et al. 2011; Harismendy et al. 2011; Paul et al. 2011). A recent study of chromatin marks in nine different cell lines produced a genome-wide map of regulatory elements and showed a twofold enrichment for predicted enhancers among the associated SNPs from GWAS (Ernst et al. 2011). These examples illustrate the power of combining statistical associations between a region of the genome and a phenotype together with functional data in order to generate hypotheses about the mechanism underlying the association.

The main goal of the Encyclopedia of DNA Elements (ENCODE) project is to identify all functional elements in the human genome, including coding and noncoding transcripts, marks of accessible chromatin, and protein binding-sites (The ENCODE Project Consortium 2004, 2007, 2011). The data sets generated by the ENCODE Consortium are therefore particularly well suited for the functional interpretation of GWAS results. To date, a total of 147 different cell types have been studied using a wide variety of experimental assays (The ENCODE Project Consortium 2012). Chromatin accessibility has been studied using DNase-seq, which led to the identification of 2.89 million DNase I–hypersensitive sites that may exhibit regulatory function. DNase footprinting (Hesselberth et al. 2009; Boyle et al. 2011; Pique-Regi et al. 2011) was used to detect binding between proteins and the genome at a nucleotide resolution. ChIP-seq experiments were conducted for a total of 119 transcription factors and other DNA-binding proteins. Together these data provide a rich source of information that can be used to associate GWAS annotations with functional data.

In this work, we show that data generated by the ENCODE Consortium can be successfully used to functionally annotate associations previously identified in genome-wide association studies. We combine multiple sources of evidence in order to identify SNPs that are located in a functional region of the genome and are associated with a phenotype. We show that a majority of known GWAS associations overlap a functional region or are in strong linkage disequilibrium with a SNP overlapping a functional region. We find that for a majority of associations, the SNP whose functional role is most strongly supported by ENCODE data is a SNP in linkage disequilibrium with the reported SNP, not the genotyped SNP reported in the association study. We show that there is significant overall enrichment for regulatory function in disease-associated regions and that combining multiple sources of evidence leads to stronger enrichment. We use information from RegulomeDB (Boyle et al. 2012), a database designed for fast annotation of SNPs that combines ENCODE data sets (ChIP-seq peaks, DNase I hypersensitivity peaks, DNase I footprints) with additional data sources (ChIP-seq data from the NCBI Sequence Read Archive, conserved motifs, eQTLs, and experimentally validated functional SNPs). Using these publicly available resources makes the approach presented herein easily applicable to the analysis of any future GWAS study.

Results

We use linkage disequilibrium information in order to integrate GWAS results with ENCODE data and eQTLs. We call *functional SNP* any SNP that appears in a region identified as associated with a biochemical event in at least one ENCODE cell line. Functional SNPs can be further subdivided into SNPs that overlap coding or noncoding transcripts, and SNPs that appear in regions identified

as potentially regulatory, such as ChIP-seq peaks and DNase I–hypersensitive sites. We call the SNPs that are reported to be statistically associated with a phenotype *lead SNPs*. For each lead SNP, we first determine whether the lead SNP itself is a functional SNP, then find all functional SNPs that are in strong linkage disequilibrium with the lead SNP. We integrate eQTL information in a similar way, by checking whether the lead SNP or a SNP in strong linkage disequilibrium with the lead SNP has been associated with a change in gene expression.

Figure 1 illustrates our approach by describing a scenario in which a lead SNP is in strong linkage disequilibrium with a functional SNP that overlaps a transcription factor binding site, as well as with a third SNP that is an eQTL. If neither the lead SNP nor the eQTL SNP overlaps a functional region, then the functional SNP is more likely to be the SNP that plays a biological role in the phenotype than either of the SNPs that were genotyped. An extreme example would be the case in which all three SNPs are in perfect linkage disequilibrium, but only the associated SNP was present on the genotyping platform used in the GWAS in which the association was found, and only the eQTL SNP was present on the genotyping platform used in the eQTL study. In this scenario, the functional SNP would be associated equally strongly with the disease and with the change in gene expression than the reported association and eQTL SNPs, respectively. To show the potential of this approach, we analyze a set of 5694 curated associations from the NHGRI GWAS catalog (Hindorff et al. 2009) that represent
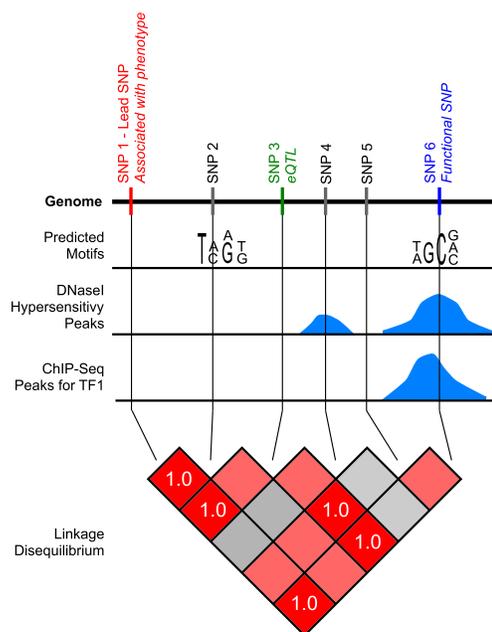
Figure 1. Schematic overview of the functional SNP approach. This figure illustrates the approach we use to identify functional SNPs. Three different types of regulatory data are represented for an area of the genome: motif-based predictions, DNase I hypersensitivity peaks, and ChIP-seq peaks. This region contains six SNPs. SNP1 is associated with a phenotype in a genome-wide association study. SNP3 is an eQTL associated with changes in gene expression in a different study. SNP6 overlaps a predicted motif, a DNase I hypersensitivity peak, and a ChIP-seq peak. There are, therefore, multiple sources of evidence that SNP6 is in a regulatory region. Furthermore, SNP6 is in perfect linkage disequilibrium ($r^2 = 1.0$) with SNP1 and SNP3, meaning that there is transitive evidence due to the LD that SNP6 is also associated with the phenotype and is also an eQTL. SNP6 is therefore the most likely functional SNP in this associated region.

a total of 4724 distinct SNPs associated with a total of 470 different phenotypes (for details, see Methods).

Lead SNP annotation

We first annotated each lead SNP with transcription information from GENCODE v7 and regulatory information from RegulomeDB. Overall, 44.8% of all lead SNPs overlap with some ENCODE data, making them functional SNPs according to our definition, and 13.1% of the lead SNPs are supported by more than one type of functional evidence. Specifically, 223 lead SNPs (4.7%) overlap coding regions, 146 (3.1%) overlap with the noncoding part of an exon, 1714 (36.3%) overlap with a DNase I peak in at least one cell line, 355 (7.5%) overlap with a DNase I footprint, and 938 (19.9%) overlap with a ChIP-seq peak for at least one of the assessed proteins in at least one cell line. Figure 2 shows the fraction of lead SNPs supported by different sources of evidence. Thus, we find that many GWAS SNPs overlap ENCODE data.

Linkage disequilibrium

For each lead SNP, we next located the set of SNPs that are in strong linkage disequilibrium ($r^2 \geq 0.8$) with the lead SNP in all four HapMap 2 populations, and annotate each SNP in this set. As expected, the fraction of lead SNPs in strong linkage disequilibrium with a SNP overlapping each type of functional evidence is larger than when considering lead SNPs alone (Fig. 2), and 58% of all associations are in strong linkage disequilibrium with at least one functional SNP. A similar increase can be observed for functional SNPs supported by multiple sources of evidence. We repeated the same analysis for the 2464 lead SNPs that have been associated with a phenotype in a population of European descent, using SNPs in strong linkage disequilibrium ($r^2 \geq 0.8$) with the lead SNP in the European HapMap population only. A total of 81% of the lead SNPs are in strong LD with at least one functional SNP, and 59% of the associated SNPs are in strong linkage disequilibrium with a functional SNP supported by multiple sources of evidence

(Fig. 2B). A detailed breakdown for each type of functional evidence for multiple linkage disequilibrium thresholds is provided in Supplemental Tables 2 and 3.

Integrating gene expression data

We integrated data from multiple eQTL studies that identified SNPs associated with changes in gene expression in several tissues. A total of 462 lead SNPs (9.8%) are also themselves an eQTL in at least one tissue, and an additional 135 lead SNPs (2.8%) are in strong LD ($r^2 \geq 0.8$ in all HapMap 2 populations) with an eQTL. When considering only associations in populations of European descent, 483 lead SNPs (19.6%) are either an eQTL, or in strong LD with an eQTL. We observe that among lead SNPs that are also eQTLs, the fraction that overlaps DNase I peaks (201, 43.5%) and ChIP-seq peaks (118, 25.5%) is significantly higher than when considering all lead SNPs (P-values of 7.6×10^{-4} and 1.7×10^{-3}, respectively).

SNP comparison within linkage disequilibrium regions

ENCODE data can be used in order to compare multiple functional SNPs that are in LD with a given lead SNP. We used a two-step approach to compare the functional annotation of two SNPs. First, if one of the SNPs is in a coding region according to GENCODE v7 and the other one is not, the coding SNP is considered to be more likely to be functional. Similarly, a SNP in a noncoding part of an exon is considered to be more likely to be functional than a SNP in an intergenic region or an intron. Second, if both SNPs are not in exons, then we compared the amount of evidence across data sources supporting the functional role of the SNP using a scoring scheme integrated in RegulomeDB (see Supplemental Methods). We hypothesized that a SNP supported by multiple types of evidence (e.g., a ChIP-seq peak and a DNase I footprint) is more likely to be functional than a SNP supported by a single experimental modality. We find that most associations where the lead SNP is in LD with at least one other SNP, the SNP with the most strongly
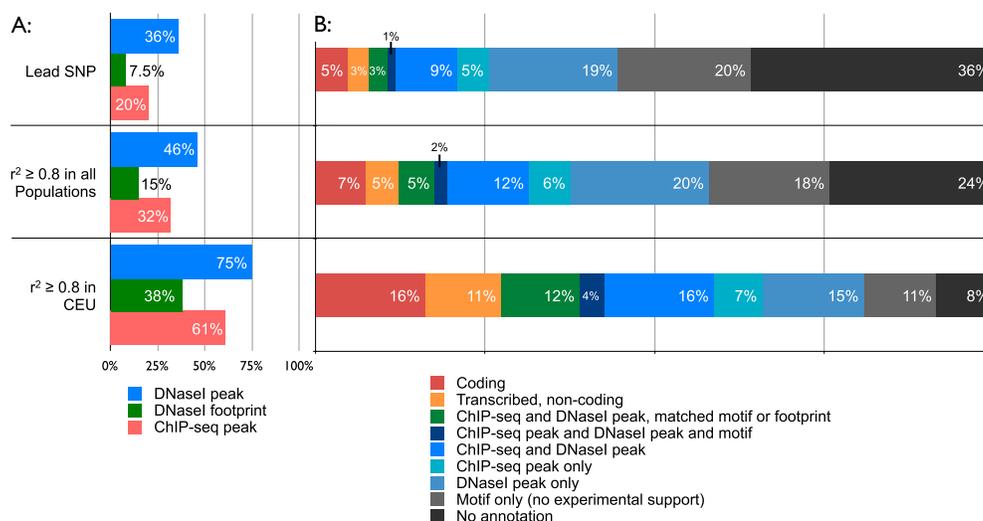
Figure 2. Proportions of associations for different types of functional data. Proportions are shown for individual assays (A) and for all sources of evidence combined (B). Proportions are presented separately for lead SNPs and SNPs in strong linkage disequilibrium ($r^2 \geq 0.8$) with a lead SNP. For each association, we determine which SNP in the LD region is most strongly supported by functional data in order to generate the proportions in panel B. We separately consider SNPs in strong linkage disequilibrium with a lead SNP in all HapMap 2 populations, and SNPs in strong linkage disequilibrium with a lead SNP in the CEU population. For the latter case, we use only associations identified in populations of European descent, and show that we can map 80% of these associations to a functional SNP supported by experimental ENCODE data.

supported functional SNP is not the lead SNP itself, but another SNP in the LD region (22.4% compared with 13.6% when using LD in all populations, 56.8% compared with 13.6% percent when considering CEU only) (Table 1). These results show that, in most cases, the associated SNP reported in a GWAS is not the most likely to play a biological role in the phenotype according to ENCODE data.

Associations are enriched for regulatory elements

We performed randomizations in order to compare the fraction of lead SNPs that are functional SNPs or are in linkage disequilibrium with a functional SNP, to the expected fraction among all SNPs. We found that associated regions are significantly enriched for functional SNPs identified using DNase-seq and ChIP-seq. Furthermore, enrichments increased, both when integrating multiple ENCODE assays and when adding eQTL information. We used a subset of 2364 lead SNPs for which sufficient information is available and built 100 random matched SNP sets in which each lead SNP is replaced by a similar SNP (for details, see Methods). We compared the fraction of lead SNPs overlapping functional regions in the set of actual lead SNPs with the fractions observed in the random sets and computed enrichment values in order to show that the fraction of associated SNPs that overlap functional regions is higher than expected. Figure 3 provides an overview of the enrichment for different types of functional data.

When considering lead SNPs only, we observed a 1.12-fold enrichment for DNase peaks, a 1.22-fold enrichment for DNase footprints, and a 1.25-fold enrichment for ChIP-seq peaks. All enrichments are statistically significant (P-values of 1.3×10^{-4}, 0.005, and 1.3×10^{-6}, respectively). We also observed that combining multiple types of evidence increases the enrichment: There is a 1.36-fold enrichment for lead SNPs that overlap with a ChIP-seq peak, a DNase peak, a DNase footprint, and a predicted motif. Similarly, there is an 1.33-fold enrichment for eQTLs, and an even higher enrichment for eQTLs that also overlap functional regions (up to 2.4-fold).

Figure 3. Overview of enrichment for different combinations of assays. Enrichments are reported for all lead SNPs associated with a phenotype and separately for lead SNPs that are also eQTLs or in strong linkage disequilibrium with an eQTL. The enrichment for predicted motifs alone (italics) is not significant. These results show that combining multiple types of experimental evidence increases the observed enrichment.

In a similar way, limiting the set of lead SNPs to the most strongly supported associations (replication in a different cohort in the original study or in multiple studies) leads to an increase in enrichment (Supplemental Fig. 1C). The enrichments can be compared with the 1.05-fold enrichment (not significant, P-value 0.087) observed when considering overlap with motif-based predictions, which do not make use of ENCODE data. When extending the set of possible functional SNPs to SNPs that are in linkage disequilibrium with a lead SNP, we observed a decrease in the enrichment (Supplemental Fig. 1A,B). At an r^2 LD threshold of 0.8, enrichments for most individual modalities are barely significant, but enrichment for functional SNPs supported by multiple sources of evidence remains significant (Supplemental Tables 3, 4).

Analysis at the phenotype level

In addition to considering individual associations separately, we can group associated SNPs in order to search for patterns at the phenotype level. We first assessed whether there are specific sequence binding proteins that tend to overlap functional SNPs associated with certain phenotypes more often than expected, using only associations in populations of European descent (Fig. 4). We found a strong association (P-value = 9×10^{-5}) between height and *CTCF* ChIP-seq peaks. A total of 39 SNPs associated with height overlap a ChIP-seq peak or are in strong linkage disequilibrium ($r^2 \geq 0.8$ in the CEU population) with a SNP that overlaps a ChIP-seq peak, and 15 of those (38%) overlap a peak for *CTCF* (Supplemental Table 5), compared with 89 out of 626 SNPs (14%) when considering all phenotypes. We also found an interesting interaction between prostate cancer and the androgen receptor (*AR*), a transcription factor that was not assessed by ENCODE but as a control in a separate study (Wei et al. 2010). Of the nine functional SNPs for prostate cancer that overlap a ChIP-seq peak, five overlap an *AR* ChIP-seq peak (Supplemental Table 5). A similar analysis using DNase I assays shows that some cell line– and tissue-specific

Table 1. Comparison of functional evidence between the lead SNP and the best SNP in the linkage disequilibrium region

	All populations		CEU only	
Only lead SNP coding	199	4.21%	87	3.53%
Only lead SNP transcribed, noncoding	113	2.39%	39	1.58%
Lead SNP supported by more regulatory evidence	329	6.96%	208	8.44%
Lead better	**641**	**13.56%**	**334**	**13.56%**
Lead SNP and SNP in LD coding	24	0.51%	48	1.95%
Lead SNP and SNP in LD transcribed, noncoding	21	0.44%	30	1.22%
Lead SNP and SNP in LD have similar regulatory evidence	282	5.97%	193	7.83%
Lead and SNP in LD equal	**327**	**6.92%**	**271**	**11.00%**
Lead SNP transcribed, noncoding, SNP in LD coding	12	0.25%	17	0.69%
Lead SNP not transcribed, SNP in LD coding	110	2.33%	244	9.90%
Lead SNP not transcribed, SNP in LD transcribed, noncoding	98	2.07%	207	8.40%
SNP in LD supported by more regulatory evidence	356	7.53%	456	18.51%
SNP in LD annotated, lead SNP not annotated	483	10.22%	476	19.32%
SNP in LD better	**1059**	**22.40%**	**1400**	**56.82%**
No annotation	1147	24.26%	208	8.44%
Lead SNP annotated, no SNP in LD	1553	32.85%	251	10.19%

When considering a linkage disequilibrium threshold in the CEU population alone, only associations that were identified or replicated in populations of European descent are used. Boldfaced text indicates the summary of each section.
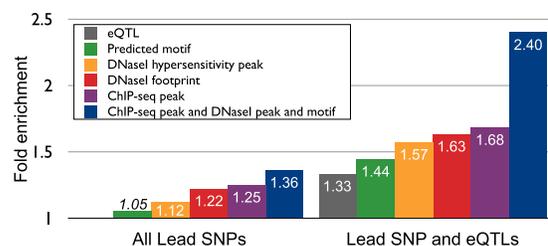
Phenotype	Total Lead SNPs	Overlap with any ChIP-seq data set	POLR2A	HNF4A	CTCF	CEBPB	EP300	RFX3	SP1	STAT3	FOXA1	GATA2	RAD21	GATA1	JUND	JUN	MYC	FOS	MAFK	NFKB1	MAX	USF1	YY1	AR	EBF1	CDX2	ZNF263	SMC3	ELF1	SP1	IKZF1	TCF4	TBP	FOXA2	TAL1	PAX5	GATA3	CREBBP	TRIM28	ETS1	USF2	BATF	SMARCA4	ESR1	TFAP2C
Total	2364	626	109	90	89	74	69	66	58	54	51	51	51	50	48	44	43	42	42	40	38	33	32	31	31	30	30	29	28	28	27	27	27	26	25	25	24	23	22	22	22	21	20	20	20
Height	112	39	6	4	**15**	7	4	5	4	5	4	3	7	3	6	4	2	5	2	5	2	3	5	0	3	1	2	6	3	3	1	1	2	3	1	1	1	0	2	1	1	1	2	1	0
Coronary heart disease	55	15	2	1	4	1	3	0	1	2	1	1	0	1	0	0	1	0	0	2	1	1	0	0	2	0	0	1	1	1	1	1	0	1	1	0	1	0	1	0	1	0	1	0	1
Type 2 diabetes	43	12	3	1	4	2	3	2	2	2	1	2	1	1	2	2	1	1	2	1	0	2	0	0	1	0	0	2	0	0	0	1	0	0	1	0	1	0	0	0	0	0	2	0	0
Cognitive test performance	39	5	0	0	1	0	0	0	0	0	0	1	1	0	0	0	1	0	0	0	0	0	0	0	0	1	0	0	0	1	0	0	0	0	1	0	0	0	0	0	0	1	1	0	0
Bipolar disorder	39	7	0	2	1	0	0	0	1	0	1	0	0	0	0	0	0	0	0	1	0	0	0	0	1	0	0	0	0	0	1	0	1	0	0	0	0	0	1	1	0	0	0	0	0
Body mass index	39	12	1	0	1	3	1	3	1	1	0	0	0	0	0	0	0	0	1	0	1	0	0	0	1	0	0	0	0	0	0	0	0	0	0	1	1	1	1	2	0	0	0	0	0
Ulcerative colitis	38	14	1	2	1	1	1	1	0	1	0	1	0	1	0	1	1	0	2	0	1	0	1	1	0	2	0	0	1	1	0	0	0	0	0	0	2	0	1	0	0	0	1	0	0
Bipolar disorder and schizophrenia	36	8	0	1	1	1	0	0	1	0	1	1	0	0	0	1	0	1	0	0	0	0	1	1	1	1	0	0	2	0	0	0	0	0	0	0	1	0	1	0	0	0	1	0	0
Crohn's disease	33	12	6	3	2	3	4	2	0	1	1	2	2	4	4	3	4	1	1	3	3	1	0	0	3	1	1	1	2	2	1	0	2	0	1	0	2	0	1	0	2	2	1	1	1
Systemic lupus erythematosus	31	9	3	1	0	0	1	2	3	0	0	0	1	0	0	2	0	0	4	2	1	2	0	1	0	0	1	1	0	1	1	0	2	0	0	1	1	0	2	2	1	1	1	1	1
Sudden cardiac arrest	31	10	2	3	2	0	1	1	1	1	0	1	0	0	0	0	0	0	2	0	0	0	1	0	0	1	1	0	1	1	0	1	1	1	0	0	0	0	1	0	0	0	1	0	1
Menarche (age at onset)	31	5	2	0	2	1	0	1	1	1	0	0	1	1	0	1	0	0	0	1	0	0	0	1	1	0	0	1	1	0	0	1	0	0	0	0	1	0	2	0	0	1	0	1	0
Cognitive performance	30	5	1	1	0	0	0	0	0	1	0	0	0	0	1	0	0	0	0	0	0	0	0	0	0	0	0	1	0	0	0	0	0	0	0	0	1	0	0	0	0	0	0	0	0
Type 1 diabetes	29	10	2	1	1	1	0	1	0	1	1	0	0	0	0	0	0	0	1	1	1	0	1	0	1	0	1	0	1	1	0	0	1	0	0	0	0	0	1	0	1	0	0	0	0
Attention deficit hyperactivity disorder	29	6	0	0	1	2	0	1	0	0	0	0	0	0	0	0	0	0	0	1	0	0	0	0	1	0	0	0	0	0	1	0	0	0	0	0	1	0	1	0	0	0	0	0	0
Prostate cancer	28	9	2	1	0	0	2	1	0	0	0	3	0	2	1	1	2	2	1	0	1	1	0	**5**	0	0	0	0	0	0	0	0	0	0	0	0	2	0	1	0	0	0	0	0	0
Breast cancer	26	11	3	0	3	2	2	2	2	1	4	2	2	1	0	3	1	2	1	2	1	0	1	0	0	0	2	1	1	1	1	0	1	3	0	0	1	0	0	1	0	1	0	1	1	1
Protein quantitative trait loci	25	7	2	0	1	0	1	0	0	2	0	0	0	0	1	1	0	1	0	1	0	1	0	0	1	0	0	2	1	0	0	1	0	0	0	0	0	0	1	0	0	1	0	0	0
Response to statin therapy	25	4	0	1	1	1	0	0	0	1	0	1	1	1	1	0	0	0	0	1	0	1	0	0	0	0	0	0	0	0	0	0	0	0	0	0	0	0	0	0	0	0	0	0	0
Amyotrophic lateral sclerosis	24	2	0	0	0	0	0	0	0	1	0	0	0	0	0	0	1	0	0	1	0	0	0	0	0	0	0	0	0	0	0	0	0	0	0	0	0	0	0	0	0	0	0	0	0
Response to antipsychotic treatment	23	3	1	0	1	0	0	0	0	0	0	0	0	0	0	0	0	0	0	0	0	0	0	0	1	0	0	0	0	1	0	0	0	0	0	0	0	0	1	0	0	0	0	0	0
Rheumatoid arthritis	23	11	1	1	1	0	3	1	1	0	0	1	1	0	0	1	1	0	2	1	1	2	1	1	0	0	1	1	0	0	0	1	0	0	0	1	1	1	0	0	2	0	0	1	1
Hematological and biochemical traits	23	7	1	2	1	1	1	0	0	0	2	1	1	1	0	1	1	0	1	0	1	1	0	0	0	0	1	0	0	0	2	1	0	1	0	0	0	0	0	1	0	0	0	0	0
Longevity	22	4	0	1	1	0	0	0	1	0	0	1	0	0	0	0	0	0	0	0	0	0	0	0	1	0	0	0	0	0	0	1	0	0	0	0	0	0	0	0	0	0	0	0	0
QT interval	22	5	0	0	1	0	0	1	1	0	0	1	1	0	0	0	0	0	0	0	0	0	0	0	0	0	0	1	0	0	0	0	0	0	0	0	0	0	0	0	0	0	0	0	0
Information processing speed	20	5	0	1	0	1	3	1	1	1	0	0	0	1	0	0	0	1	0	1	0	1	0	0	0	0	0	0	1	0	0	0	0	0	0	0	1	0	0	0	0	1	1	0	0
Multiple sclerosis	20	5	1	2	1	2	1	0	0	0	2	1	0	1	0	2	1	0	0	0	1	1	0	0	0	0	1	0	0	0	1	0	0	0	0	0	1	0	0	0	0	0	0	0	0
Quantitative traits	20	3	1	0	1	0	0	0	1	0	0	1	1	1	0	0	1	0	0	0	0	0	0	0	0	0	0	1	0	0	0	0	0	0	0	0	1	0	0	0	0	0	1	0	0

Figure 4. Phenotype level overview of the overlap between associations and ChIP-seq binding. This matrix view shows phenotypes vertically and DNA binding proteins assessed using ChIP-seq horizontally. Each cell represents the number of lead SNPs for the respective phenotype that overlap with a ChIP-seq peak for the respective DNA binding protein or are in strong LD ($r^2 \geq 0.8$ in the CEU HapMap 2 population) with a SNP that overlaps such a peak. Only phenotypes with at least 20 lead SNPs and DNA binding proteins overlapping at least 20 functional SNPs are shown, but totals are computed over the entire data set. The significant interaction between height-associated functional SNPs and *CTCF*, as well as the association between prostate cancer–associated functional SNPs and androgen receptor (*AR*), are represented in bold font.

binding patterns can be observed for certain phenotypes, however, without reaching statistical significance (Supplemental Fig. 2).

Specific examples

We identified functional SNPs in strong linkage disequilibrium for a large fraction of all reported associations. A table mapping each association to a list of candidate functional SNPs is available on our website (http://RegulomeDB.org/GWAS) and as online Supplemental Materials. Table 2 highlights the lead SNPs supported by the strongest functional evidence. These overlap a ChIP-seq peak, a DNase peak, a DNase footprint, and a predicted motif, and the transcription factor binding detected using ChIP-seq matches the conserved motif used in DNase footprinting. Table 3 provides a similar list for functional SNPs supported by the same amount of

regulatory evidence, but that are in strong LD with a lead SNP. The lead SNP itself is supported by less or no evidence of a functional role. Functional SNPs in strong LD with the lead SNP are located as far as 170 kb from the reported association. Each of the functional SNPs we identify is a biological hypothesis supported by experimental regulatory data, but that still requires further validation. In this section, we describe several functional SNPs in more detail and show how ENCODE data can be used to generate interesting biological hypotheses.

First, we show that we can re-identify a previously validated functional SNP. Lead SNP rs1541160 is associated with amyotrophic lateral sclerosis (ALS) in a GWAS, and there is no evidence that this SNP overlaps a functional region. However, it is in perfect LD with rs522444, a functional SNP overlapping DNase hypersensitivity regions and ChIP-seq peaks in a large number of ENCODE

Table 2. Overview of the lead SNPs that are most strongly supported by functional evidence

	Lead SNP	Lead SNP score	Phenotype	PubMed ID	Rep	*P*-value
chr1	rs1967017	2a	Serum urate	20884846	Yes	4×10^{-8}
chr5	rs2188962	2a	Crohn's disease	20570966	Yes	1×10^{-7}
			Crohn's disease	18587394	Yes	2×10^{-18}
chr6	rs9491696	2a	Waist–hip ratio	20935629	Yes	2×10^{-32}
chr6	rs9483788	2a	Hematocrit	19862010	Yes	3×10^{-15}
			Other erythrocyte phenotypes	19862010	Yes	1×10^{-47}
chr11	rs2074238	2a	QT interval	19305408	Yes	3×10^{-17}
chr11	rs7940646	2a	Platelet aggregation	20526338	Yes	1×10^{-6}
chr12	rs902774	2a	Prostate cancer	21743057	Yes	5×10^{-9}
chr14	rs1256531	2a	Conduct disorder (symptom count)	20585324		4×10^{-6}
chr15	rs17293632	2a	Crohn's disease	21102463	Yes	3×10^{-19}
chr16	rs4788084	2a eQTL	Type 1 diabetes	19430480	Yes	3×10^{-13}
chr17	rs9303029	2a	Protein quantitative trait loci	18464913		4×10^{-7}
chr19	rs10411210	2a	Colorectal cancer	19011631	Yes	5×10^{-9}
chr19	rs3764650	2a	Alzheimer's disease	21460840	Yes	5×10^{-17}

Each of these lead SNPs overlaps a ChIP-seq peak, matched DNase footprint, matched motif, and a DNase I-seq peak.

Table 3. Overview of all strongly supported functional SNPs in linkage disequilibrium with an associated lead SNP

Lead SNP	Lead SNP	Lead SNP score	Phenotype	PubMed ID	Rep	P-value	Best SNP in LD	Score	Distance to lead SNP (bp)	Linkage disequilibrium (r^2)			
										CEU	CHB	JPT	YRI
Functional SNP in LD ≥ 0.8 in all populations													
chr1	rs6686842	6	Height	18391952	Yes	2×10^{-8}	rs11209342	2a	61,205	0.96	0.90	1.00	1.00
chr1	rs380390	6	Age-related macular degeneration			4×10^{-8}	rs381974	2a	8379	1.00	0.85	1.00	1.00
chr3	rs6806528	4	Celiac disease	20190752	Yes	2×10^{-7}	rs6784841	2a	733	1.00	1.00	1.00	1.00
chr4	rs1800789	7	Fibrinogen	20031576	Yes	2×10^{-30}	rs4333166	2a	1232	1.00	1.00	1.00	1.00
chr5	rs3776331	7	Serum uric acid	18759275		8×10^{-6}	rs3893579	2a	4547	0.96	1.00	0.95	1.00
chr6	rs7743761	5b eQTL	Ankylosing spondylitis	20062062	Yes	8×10^{-303}	rs6457401	2a eQTL	1248	0.93	0.95	1.00	1.00
chr6	rs642858	6	Type 2 diabetes	21490949		2×10^{-6}	rs1361248	2a	21,711	0.94	1.00	1.00	0.92
chr7	rs12700667	4	Endometriosis	21151130	Yes	1×10^{-9}	rs1451385	2a	6918	0.85	0.92	1.00	1.00
chr9	rs3890182	5b	HDL cholesterol	20864672	Yes	5×10^{-7}	rs3847302	2a	940	1.00	1.00	1.00	0.94
			HDL cholesterol	18193044	Yes	3×10^{-10}							
chr9	rs2383207	7	Abdominal aortic aneurysm	20622881	Yes	2×10^{-8}	rs1333047	2a	8545	0.89	0.95	1.00	1.00
chr16	rs7197475	6 eQTL	Systemic lupus erythematosus	19838193	Yes	3×10^{-8}	rs7194347	2a	2777	1.00	1.00	1.00	0.83
chr16	rs7186852	5a eQTL	Systemic lupus erythematosus	19838193	Yes	3×10^{-7}	rs7194347	2a	9985	0.96	1.00	1.00	0.83
chr19	rs12986413	4	Height	18391950	Yes	3×10^{-8}	rs1015670	2a	536	1.00	1.00	1.00	0.96
Functional SNP in LD ≥ 0.8 in CEU–Association in European population													
chr1	rs2816316	7	Celiac disease	20190752	Yes	2×10^{-17}	rs2984920	2a	7982	1.00	1.00	1.00	0.05
			Celiac disease	18311140	Yes		rs1323296	eQTL	695	1.00	1.00	1.00	0.52
chr1	rs4949526	5a	Bipolar disorder and schizophrenia	20889312		4×10^{-7}	rs4949524	2a	9517	0.84	0.69	0.59	0.00
chr4	rs4234798	2b	Insulin-like growth factors	21216879		5×10^{-10}	rs4234797	2a	26	1.00	0.79	1.00	1.00
chr6	rs1361108	5b	Menarche (age at onset)	21102462	Yes	3×10^{-15}	rs9388486	2a	106,446	0.92	1.00	0.00	0.51
chr6	rs9494145	7	Red blood cell traits	20927387		3×10^{-6}	rs9483788	2a	2949	0.87	0.73	0.89	1.00
chr7	rs1055144	5b	Waist–hip ratio	20935629	Yes	1×10^{-24}	rs1451385	2a	23,612	0.83	0.17	0.11	0.02
chr8	rs2019960	7	Hodgkin's lymphoma	21037568	Yes	1×10^{-13}	rs7826019	2a	5723	1.00	0.00	0.63	0.96
chr9	rs7873102	7	Brain structure	20171287		6×10^{-7}	rs776010	2a	111,304	0.96	0.79	0.75	0.00
chr9	rs1333049	7	Coronary heart disease	21606135	Yes	7×10^{-58}	rs1333047	2a	999	1.00	0.51	0.40	0.00
			Coronary heart disease	17634449	Yes	3×10^{-19}							
			Coronary heart disease	17554300	Yes	1×10^{-13}							
chr9	rs4977574	2c	Coronary heart disease	21378990	Yes	1×10^{-22}	rs1333047	2a	25,930	0.89	0.47	0.36	0.00
			Coronary heart disease	21378988	Yes	2×10^{-25}							
			Myocardial infarction (early onset)	19198609	Yes	3×10^{-44}							
chr9	rs3905000	7	MRI atrophy measures	21116278	Yes	9×10^{-6}	rs3847302	2a	8475	1.00	1.00	1.00	0.67
			HDL cholesterol	19060911	Yes	9×10^{-13}							
chr10	rs1561570	4 eQTL	Paget's disease	21623375	Yes	4×10^{-38}	rs10752286	2a	4377	0.96	1.00	1.00	0.70
			Paget's disease	20436471	Yes	6×10^{-13}							
chr10	rs563507	5b	Acute lymphoblastic leukemia (childhood)	19684603	Yes	9×10^{-9}	rs773983	2a	38,857	1.00	0.00	0.00	0.13
chr11	rs7127900	5b	Prostate cancer	19767753	Yes	3×10^{-33}	rs7123299	2a	1230	1.00	1.00	0.89	0.65
chr11	rs561655	5b	Alzheimer's disease (late onset)	21460841	Yes	7×10^{-11}	rs1237999	2a	14,751	0.84	0.83	0.62	1.00
chr11	rs10898392	7	Height	19570815	Yes	3×10^{-6}	rs575050	2a	174,791	0.81	0.95	0.42	0.73
chr12	rs2638953	7	Height	20881960	Yes	7×10^{-17}	rs10506037	2a	116,731	0.84	1.00	1.00	0.00
chr14	rs7142002	7	Autism	20663923	Yes	3×10^{-22}	rs3993395	2a	38,489	0.87	0.26	0.20	0.62
chr15	rs261334	5b	HDL cholesterol	20864672	Yes	5×10^{-22}	rs8034802	2a	1952	0.83	0.27	0.48	0.57
chr17	rs12946454	5b	Systolic blood pressure	19430483	Yes	1×10^{-8}	rs11657325	eQTL	41,323	1.00	0.93	0.81	0.51
chr17	rs6504218	7	Coronary heart disease	21378988	Yes	1×10^{-6}	rs9902260	2a	8427	0.92	1.00	1.00	0.56
chr22	rs738322		Cutaneous nevi	21478494	Yes	1×10^{-6}	rs2016755	2a	29,402	0.89	0.71	0.44	0.71

This table represents associations for which there is more evidence supporting a regulatory role for a functional SNP in linkage disequilibrium with the lead SNP than for the lead SNP itself. Each functional SNP in this table overlaps a ChIP-seq peak, matched DNase footprint, matched motif, and a DNase I-seq peak. The table is separated into cases in which the functional SNP is in strong linkage disequilibrium ($r^2 \geq 0.8$) with the lead SNP in all HapMap 2 populations, and cases in which the functional SNP is in strong linkage disequilibrium with the lead SNP in the HapMap 2 CEU population only (and the association was identified and replicated in a population of European descent).

cell lines. The investigators in the original study identified rs522444 due to its position in a putative *SP1* binding site and experimentally validated its functional role (Landers et al. 2009) in altering the expression of the gene *KIFAP3*.

One novel functional SNP that we identify is rs7163757 (Fig. 5). This SNP is in strong LD with rs7172432, a SNP recently shown to be associated with type 2 diabetes in the Japanese population and replicated in a European population (Yamauchi et al. 2010), and associated with insulin response in the Danish population (Grarup et al. 2011). This functional SNP is supported by evidence from both DNase I hypersensitivity and ChIP-seq assays. DNase footprinting indicates that the functional SNP overlaps a potential *NFAT* binding site. Interestingly, the risk allele at rs7172432 is the common allele in the population (53%), and there is a single haplotype with frequency above 1% that includes the risk allele between the associated SNP and the functional SNP, but several alleles with high frequency that include the protective allele.

A second novel functional SNP is in the 9p21 region, a gene desert that contains multiple SNPs that are strongly associated

with several common diseases. Lead SNP rs1333049 has been associated with coronary artery disease in multiple studies in populations of European (Samani et al. 2007; The Wellcome Trust Case Control Consortium 2007; Broadbent et al. 2008; Wild et al. 2011) as well as Japanese and Korean descent (Hinohara et al. 2008; Hiura et al. 2008). In the HapMap 2 CEU population, this SNP is part of a haplotype block that includes rs10757278 and rs1333047, both of which are in perfect LD with rs1333049. There is no evidence in ENCODE supporting a functional role for rs1333049. However, both rs10757278 and rs1333047 overlap a DNase hypersensitivity peak as well as ChIP-seq peaks for *STAT1* and *STAT3* in HeLA-S3 cells. Furthermore, rs10757278 lies in a *STAT1* binding site, and rs1333047 lies in a binding site and a DNase I footprint for Interferon-stimulated gene factor 3 (*ISGF3*). Figure 6 provides an overview of this region. Although the functional role of rs10757278 has been previously reported (Harismendy et al. 2011), evidence of the functional role of rs1333047 is novel. Interestingly, while only 27 bp separates the two SNPs, they are in perfect linkage disequilibrium in the CEU population only. The frequency of the *A* allele at rs1333047 in the Yoruba in Ibadan, Nigeria (YRI) HapMap 2
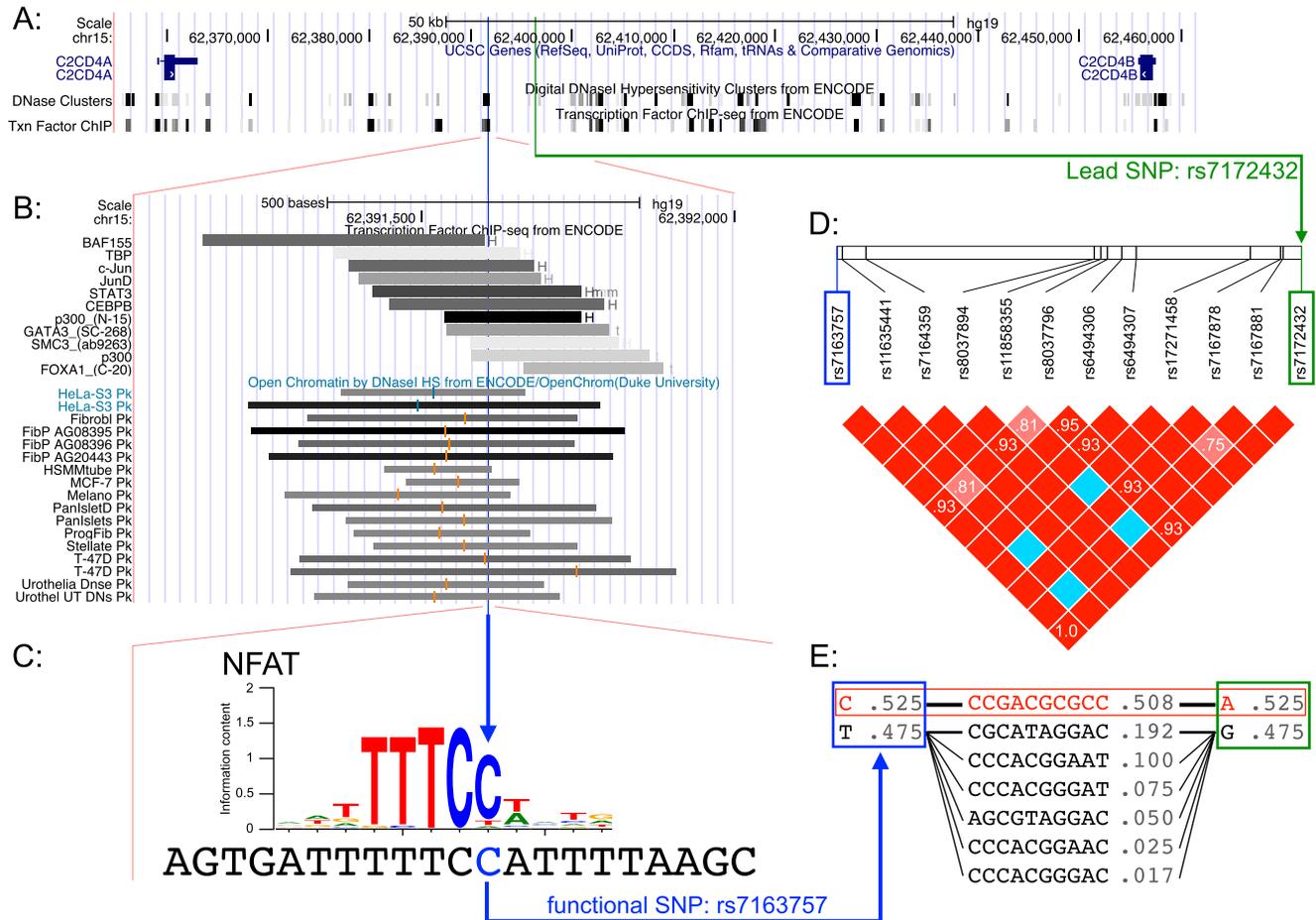
Figure 5. Functional SNP rs7163757. Multiple sources of evidence indicate that SNP rs7163757 is functional. (*A*) Overview of the region between genes *C2CD4A* and *C2CD4B*. (Blue vertical line) Functional SNP rs7163757; (green vertical line) lead SNP rs7172432. Multiple ChIP-seq and DNase-seq peaks can be seen, including one that overlaps rs71763757. (*B*) Vicinity of functional SNP rs7163757. ChIP-seq binding is observed for multiple transcription factors in multiple cell lines. Due to space, DNase peaks are represented only for a subset of the peaks overlapping the region. (*C*) Sequence around rs7163757 and motif for the *NFAT* binding site that overlaps the functional SNP. The minor allele is *T*. (*D*) Linkage disequilibrium region between the functional SNP and the lead SNP in the HapMap 2 CEU population. The two SNPs are in perfect LD ($r^2 = 1.0$). (*E*) Haplotypes between the functional SNP and the lead SNP. There is a single haplotype with frequency above 1% that carries the identified risk allele (*A* at rs7172432), whereas there are multiple haplotypes that include the protective allele. Haplotypes with frequency of <1% are not shown.
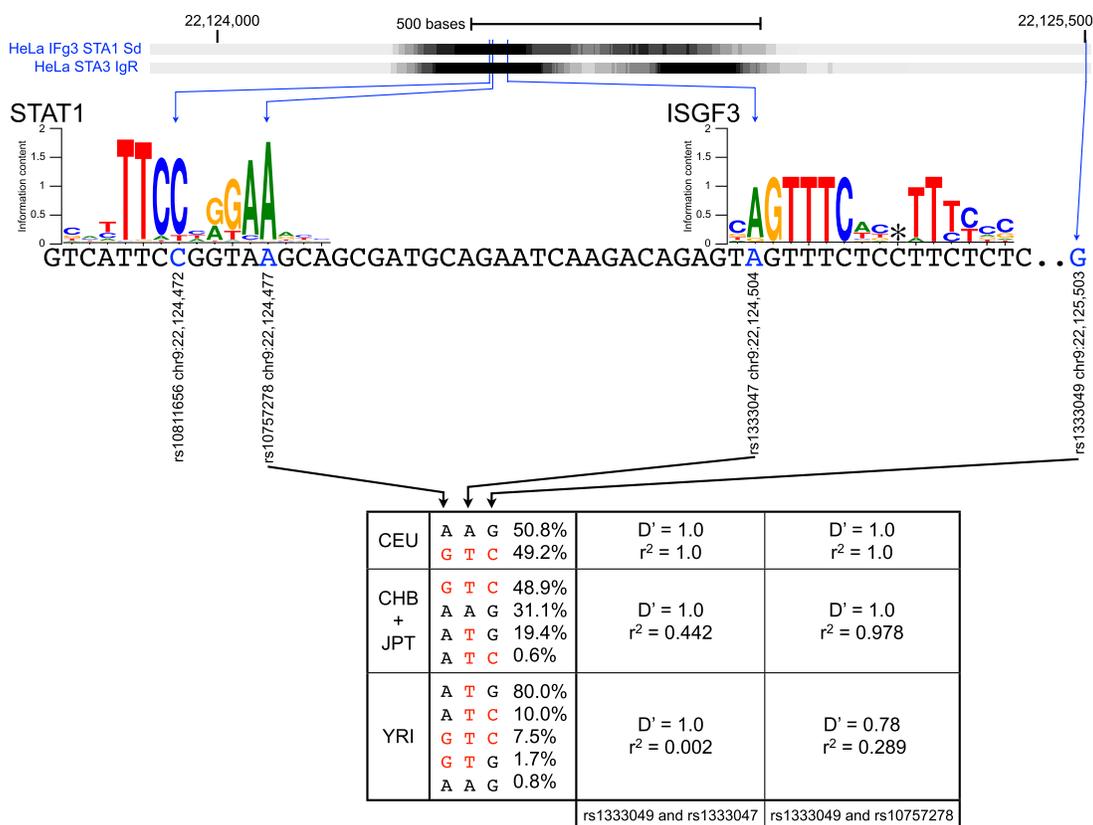
Figure 6. Functional information and linkage disequilibrium patterns support the implication of rs1333047 in coronary artery disease. Functional data (ChIP-seq) generated by the ENCODE Consortium show evidence of *STAT1* binding in the 9p21 region associated with coronary artery disease. rs10757278 and rs1333047 are both located in the peak, whereas rs1333049 is a tag SNP that does not overlap any functional region in RegulomeDB. rs10757278 is part of a regulatory motif for *STAT1* binding, and rs1333049 is part of a regulatory motif for *ISGF3* binding. (*) The location at which a gap is inserted into the motif to handle variable linker length. Haplotype frequency and linkage disequilibrium data from the different HapMap2 populations show that all three SNPs are in perfect linkage disequilibrium in the CEU population, but not the CHB and JPT populations. In the YRI population, the frequency of the *A* allele at rs1333047 is only 0.8%. Risk alleles for all SNPs are determined using the haplotype associated with coronary artery disease in the CEU population (red). There is an absence of linkage disequilibrium between rs1333047 and rs1333049 in YRI, and the association between rs1333049 and rs10757278 and coronary artery disease has not been replicated in populations of African descent.

population is only 0.8%, compared with 50.8% in the CEU population. This allele is part of the protective haplotype found in GWAS performed in populations of European descent. The *A* allele is part of the motif for *ISGF3* binding, whereas the *T* allele is not.

Discussion

In this study, we used data generated by the ENCODE Consortium to identify regulatory and transcribed functional SNPs that are associated with a phenotype, either directly in a genome-wide association study or indirectly through linkage disequilibrium with a GWAS association. We further added eQTL information, thus identifying SNPs that are associated with a phenotype, for which there is evidence that they affect a regulatory region or a transcribed region, and for which a downstream target affected by the SNP is known. This approach therefore has the potential to provide putative mechanistic explanations for GWAS associations. We showed that this method is successful in identifying a functional SNP for a majority of previously reported GWAS associations (up to 81% when considering association studies performed in populations of European descent, and using the CEU population to obtain linkage disequilibrium information).

The fraction of associated SNPs for which we can provide a functional annotation is similar to the one reported in the ENCODE integrative analysis paper (The ENCODE Project Consortium 2012). The integrative analysis uses both DNase-seq and formaldehyde-assisted isolation of regulatory elements (FAIRE) (Giresi et al. 2007) data to identify regions of open chromatin, and thus finds a slightly larger fraction of the associated SNP to overlap or be in LD with open chromatin regions compared with our approach, which does not use FAIRE data. We found that GWAS associations are significantly enriched for DNase hypersensitivity peaks, DNase I footprints, and ChIP-seq peaks even when accounting for most features of associated SNPs. Our results are consistent with chromatin state-based methods (Ernst et al. 2011), in which a segmentation approach was used in order to identify enrichment for disease associations in predicted enhancers. Segmentation-based approaches use machine learning methods to predict chromatin state at every position in the genome based mostly on histone information. These predictions are then compared with GWAS results, thus showing enrichment for predicted states. A major difference of our work is that we directly used ChIP-seq and DNase I-seq functional data in our analysis, and show enrichment for observed ChIP-seq peaks or DNase I–hypersensitive regions. In this study, we demonstrated that there is significant

enrichment of GWAS associations for these types of data. Furthermore, we found that (1) integrating multiple types of functional data and expression information identifies more likely candidate causal SNPs within an LD region, and (2) phenotypic information from GWAS studies can be associated with biochemical data.

Existing methods for prioritizing SNPs based on their functional role focused on transcribed regions (Ng and Henikoff 2003; Adzhubei et al. 2010; Saccone et al. 2010), whereas we focused on regulatory regions. In the context of regulatory regions, most approaches are based on motif information (Xu and Taylor 2009; Macintyre et al. 2010), and approaches using experimental data have generally been limited to individual associations (Harismendy et al. 2011). The comprehensive data sets generated by the ENCODE Consortium are the first to offer sufficient information to allow for genome-wide methods that rely on experimental information. We used enrichment to compare the sensitivity of our approach with motif-based methods. We found that there is no significant enrichment for GWAS associations among conserved motifs.

Identifying functional SNPs in linkage disequilibrium with lead SNPs

We found that, in most cases, there is more evidence supporting another SNP in strong LD with the lead SNP than the lead SNP itself. This is consistent with results from fine-mapping analyses that indicate that multiple variants in the linkage disequilibrium region surrounding a lead SNP appear to play a role in the phenotype of interest (Chung et al. 2011; Sanna et al. 2011). This result is of particular importance for the interpretation of GWAS results, because LD patterns differ markedly between populations. If the functional SNP is in strong LD with the lead SNP in the population in which the GWAS was performed, but not in a different population, then the lead SNP will not be associated with the phenotype in this second population. An example of this situation is functional SNP rs1333047, which lies in a region associated with coronary artery disease. This SNP is in perfect LD with two lead SNPs in populations of European descent in which the studies identifying the associations were performed, but not in populations of African descent, in which the associations could not be replicated (Assimes et al. 2008; Kral et al. 2011; Lettre et al. 2011; see Supplemental Material).

Comparison of functional assays

We integrated data from multiple types of functional assays in order to identify functional SNPs.

We found that the highest enrichments are obtained when requiring functional SNPs to be supported by multiple sources of experimental evidence rather than only one. The highest enrichments are observed when using both eQTL information and ENCODE data, and when considering associations that have been replicated. A similar trend can be observed when examining individual assays. The more specific the assay, the higher is the enrichment for overlap among GWAS associations: The DNase hypersensitivity peaks, which broadly capture regions in which chromatin is accessible, do overlap with a large fraction of SNPs in general, thus leading to relatively weak enrichments, whereas the enrichment is much higher for ChIP-seq peaks, which experimentally identify the binding of specific transcription factors and other molecules. There is a clear trade-off between the more significant enrichment we observe, and the lower fraction of associations annotated with ChIP-seq peaks. The ChIP-seq data generated

so far by the ENCODE Consortium only assesses 119 transcription factors, a fraction of the 1800 known ones (The ENCODE Project Consortium 2012). Most transcription factors are assessed in a small subset of the ENCODE cell lines, whereas DNase-seq has been performed on most ENCODE cell lines. DNase footprinting, which combines DNase-seq data with sequence and motif information, is useful to identify potential binding sites for transcription factors not assessed using ChIP-seq. An example of this situation is functional SNP rs7163757, which is in LD with a lead SNP associated with type 2 diabetes. DNase I footprinting identifies a nuclear factor of activated T-cells (*NFAT*) footprint that overlaps rs7163757. *NFAT* is part of the calcineurin/*NFAT* pathway (Crabtree and Olson 2002), which has been involved in the regulation of growth and function of the insulin-producing pancreatic beta cells, and linked to the expression of genes known to be associated with type 2 diabetes (Heit et al. 2006).

Differences between tissue types

Transcription factor binding patterns are heterogeneous and differ between tissue types. Assessing this heterogeneity has been a main motivation for the ENCODE Project. One concern is that the cell lines from which the functional information is derived do not necessarily correspond to the tissue type that is most relevant to the phenotype of interest. A similar approach has been successfully used to identify functional SNPs that play a role in coronary artery disease based on a ChIP-seq assay performed in the immortalized HeLa cell line (Harismendy et al. 2011). By choosing to use functional data across all tissues, we purposefully favor sensitivity over specificity. An example illustrating the benefits of this trade-off is rs2074238, a functional SNP associated with long QT syndrome. A ChIP-seq experiment identifies the binding of estrogen receptor alpha at this location in an epithelial cell line. Long QT syndrome is more prevalent in women (Hashiba 1978; Locati et al. 1998), the menstrual cycle affects the QT interval (Nakagawa et al. 2006), and estrogen therapy has been shown to affect the duration of the QT interval in postmenopausal women (Kadish et al. 2004; Gökçe et al. 2005). ChIP-seq data for this transcription factor are only available for two cell lines, neither of cardiac origin. By limiting our approach to functional data obtained in cardiac tissues, we would have excluded a transcription factor whose role in the phenotype is supported by extensive prior evidence. When examining all associations, the significant enrichments we report demonstrate that our current approach improves specificity compared with using motif information only.

Although the ChIP-seq data generated so far by the ENCODE Consortium are sparse, especially in terms of the number of different tissues in which a transcription factor is assessed, the number of available data sets is growing rapidly. We expect that it will soon become possible to refine this approach by considering the most relevant tissue types only, thus further improving its specificity. A remaining challenge is the identification of specific tissue types that are relevant for a given phenotype. A specific example is a functional SNP we identify in the context of Alzheimer's disease: In cell lines of hepatic origin, rs3764650 overlaps a binding site for *HNF4A*, a transcription factor known mainly to play a role in the liver. Although Alzheimer's is a neurodegenerative disease, a recently published study shows that the liver might play an important role in the disease mechanism as well (Sutcliffe et al. 2011). This example shows the benefits of looking broadly at all available experimental data from ENCODE.

Functional SNPs beyond reported associations

In this study, we focused on using ENCODE information in order to identify functional SNPs in strong LD with previously reported associations. It is, however, important to note that these SNPs only represent a small fraction of all the SNPs that overlap functional regions identified by ENCODE. SNPs that alter transcription factor binding sites are likely to have some biologically important effect and have an impact on some phenotype. Such a SNP, however, will only be found in a GWAS if the specific phenotype it affects is assessed. Given this fundamental limitation of association studies, an orthogonal approach would be to study the functional effects of common SNPs regardless of their association with a phenotype. Furthermore, this effect explains why the enrichments we observe, while significant, are relatively modest. We used a stringent null model in which a lead SNP is matched to a random SNP that is similar to the lead SNP, and in particular located at a similar distance to the nearest transcription start site. Associated SNPs are located more closely to genes than SNPs in general, and therefore null sets are also biased toward SNPs that are likely to have some biological effect. Relaxing the null model leads to higher enrichments (Supplemental Fig. 1B,C).

Conclusion

We show that genome-wide experimental data sets generated by the ENCODE Consortium can be successfully used to provide putative functional annotations for the majority of the GWAS associations reported in the literature. The use of these experimental assays outperforms the use of in silico binding predictions based on sequence motifs when trying to identify functional SNPs associated with a phenotype in a GWAS. We demonstrate that an integrative approach combining genome-wide association studies, gene expression analysis, and experimental evidence of regulatory activity leads to the identification of loci that are involved in common diseases, and generates hypotheses about the biological mechanism underlying the association. In the majority of cases, the SNP most likely to play a functional role according to ENCODE evidence is not the reported association, but a different SNP in strong linkage disequilibrium with the reported association. Our approach, which builds directly on the publicly available RegulomeDB database, provides a simple framework that can be applied to the functional analysis of any genome-wide association study.

Methods

Data

We use the NHGRI GWAS catalog (Hindorff et al. 2009) (http://www.genome.gov/gwastudies downloaded on August 10, 2011) to obtain a list of GWAS associations. We use HapMap version 2 (The International HapMap Consortium 2007) and version 3 (The International HapMap Consortium 2010) in order to obtain linkage disequilibrium information between SNPs. HapMap data can be downloaded from http://hapmap.ncbi.nlm.nih.gov/. We use the list of SNPs that appear on genotyping arrays from the *SNP Genotyping Array* track of the UCSC Genome Browser (Kent et al. 2002). We use the function information generated by the UCSC Genome Browser for each SNP in dbSNP 132 (Sayers et al. 2012). We used the November 7, 2011 version of RegulomeDB (Boyle et al. 2012) in order to annotate SNPs with regulatory information and to obtain a list of eQTL. The RegulomeDB server is available at http://www.regulomedb.org, and all ENCODE data sets used in RegulomeDB can be accessed via the ENCODE portal at http://encodeproject.org. We use GENCODE v7 (Harrow et al. 2012) to identify SNPs that overlap transcribed regions. The GENCODE v7 track can be accessed on the UCSC Genome Browser at http://genome.ucsc.edu. These data sets are described in more detail in the Supplemental Material.

Annotation

Lead SNPs

We call the associated SNP reported in a GWAS the *lead SNP*. For each lead SNP, we retrieve the regulatory annotation from RegulomeDB and the transcriptional annotation from GENCODE v7. We determine the fraction of lead SNPs that are coding, in noncoding parts of exons, that overlap DNase I peaks, DNase I footprints, and ChIP-seq peaks independently of each other. This means that if, for example, a SNP overlaps both a DNase peak and a ChIP-seq peak, then it will be counted for both types of assays. We consider that there is an overlap between the SNP and the type of assay if there is one ENCODE cell line in which there is, respectively, a DNase peak, a DNase footprint for at least one motif, or a ChIP-seq peak for at least one binding protein that overlaps the SNP. To determine a score for lead SNPs, we first assess whether the SNP is in an exon. If the SNP is not in an exon, then we assign the modified RegulomeDB score to this SNP (see the Supplemental Material). We use Fisher's exact test on a 2×2 table to compute a *P*-value for the difference in the fraction of functionally annotated SNPs between all lead SNPs and lead SNPs that are eQTLs.

Linkage disequilibrium

For each lead SNP, we compute the set of all SNPs in LD with that lead SNP. We first use an r^2 threshold in order to limit the LD set to SNPs in strong LD with the lead SNP. To add a SNP to the LD set, we require that the r^2 is above the threshold in all four HapMap 2 populations. We then look separately at associations found in populations of European descent. For each of these lead SNPs, we obtain a set of SNPs in LD with the lead SNP when considering the HapMap 2 CEU population only. We separately analyze the set of all lead SNPs, and the subset of European-descent lead SNPs.

To compute the fraction of SNPs in LD with a lead SNP that overlap a type of functional data, we do count every lead SNP at most once, namely, when one or more SNPs in the LD set overlap with the functional data type. To compute a score, we find the best candidate in the LD set corresponding to each lead SNP. We consider that a coding SNP had more functional evidence than a SNP in a noncoding part of an exon, and that a SNP in an exon has more functional evidence than a regulatory SNP. If no SNP in the LD set is transcribed, then we find the SNP with the best RegulomeDB score. We consider an associated region to be an eQTL if there is at least one eQTL in the set of SNPs in LD with the lead SNP.

Randomization

We create $n = 100$ null sets in which each lead SNP is matched to a random SNP that has a similar minor allele frequency, is present on the same genotyping platform as the lead SNP, has the same predicted function (using UCSC gene predictions), and is located at a similar distance from the nearest transcription start site. To perform these randomizations, we filter out lead SNPs for which insufficient information is available, lead SNPs that are not assessed in one or more HapMap populations, and lead SNPs that are in linkage disequilibrium with another lead SNP that is more strongly associated with a phenotype. The filtering and randomization steps are described in more detail in the Supplemental Material.

We then repeat the annotation steps on each null set and obtain an empirical distribution of the fraction of functional SNPs expected for matched SNPs, and of the score distribution among matched SNPs. We obtain a P-value for the difference between the lead SNPs and the null sets using a Student's t distribution with $n - 1$ degrees of freedom and the same mean and standard deviation from the empirical distribution of the counts overlapping the feature in the n randomized null sets. This distribution is used to estimate the probability of having a null set (which is by construction of the same size as the set of lead SNPs) with a fraction of SNPs overlapping the feature that is as extreme or more extreme than the fraction observed for the lead SNP set, which results in a two-tailed P-value.

Analysis at the phenotype level

We group all lead SNPs per phenotype using the GWAS catalog phenotype classification. We do not further group phenotypes, even though some are similar. We use only associations identified or replicated in populations of European descent. For each lead SNP, we count how many times the lead SNP or at least one SNP in strong LD ($r^2 \geq 0.8$ in the HapMap 2 CEU population) overlaps with a ChIP-seq peak for a given DNA binding protein. Each lead SNP is counted at most once for each DNA binding protein, and we ensure that no two lead SNPs are in LD with each other. We then add the totals for all of the lead SNPs associated with each phenotype. We use a Fisher's exact test on a 2×2 table to show that the fraction of lead SNPs associated with heights that are in strong LD with at least one SNP overlapping with a *CTCF* ChIP-seq peak is higher than the same fraction for all associated lead SNPs.

Analysis of individual loci

We use Haploview (Barrett et al. 2005) to analyze linkage disequilibrium data and haplotype frequencies in individual regions. We obtain transcription factor binding motifs from TRANSFAC (*STAT1*, *NFAT*) and JASPAR (*ISGF3*). The motif representations in Figures 5 and 6 were created using WebLogo 3 (Crooks et al. 2004).

Data access

The list of all functional SNP predictions we generate is available at http://RegulomeDB.org/GWAS and as online Supplemental Material.

Competing interest statement

M.S. is a consultant for Illumina, a founder and member of the scientific advisory board for Personalis, and a member of the scientific advisory board for GenapSys. S.B. is a founder of DNAnexus and a member of the scientific advisory boards of 23andMe, GigaGen, and Molecular.

Acknowledgments

References

Adzhubei IA, Schmidt S, Peshkin L, Ramensky VE, Gerasimova A, Bork P, Kondrashov AS, Sunyaev SR. 2010. A method and server for predicting damaging missense mutations. *Nat Methods* **7:** 248–249.

Assimes TL, Knowles JW, Basu A, Iribarren C, Southwick A, Tang H, Absher D, Li J, Fair JM, Rubin GD, et al. 2008. Susceptibility locus for clinical and subclinical coronary artery disease at chromosome 9p21 in the multi-ethnic ADVANCE study. *Hum Mol Genet* **17:** 2320–2328.

Barrett JC, Fry B, Maller J, Daly MJ. 2005. Haploview: Analysis and visualization of LD and haplotype maps. *Bioinformatics* **21:** 263–265.

Boyle AP, Davis S, Shulha HP, Meltzer P, Margulies EH, Weng Z, Furey TS, Crawford GE. 2008. High-resolution mapping and characterization of open chromatin across the genome. *Cell* **132:** 311–322.

Boyle AP, Song L, Lee BK, London D, Keefe D, Birney E, Iyer VR, Crawford GE, Furey TS. 2011. High-resolution genome-wide in vivo footprinting of diverse transcription factors in human cells. *Genome Res* **21:** 456–464.

Boyle AP, Hong EL, Hariharan M, Cheng Y, Schaub MA, Kasowski M, Karczewski KJ, Park J, Hitz BC, Weng S, et al. 2012. Annotation of functional variation in personal genomes using RegulomeDB. *Genome Res* (this issue). doi: 10.1101/gr.137323.112.

Broadbent HM, Peden JF, Lorkowski S, Goel A, Ongen H, Green F, Clarke R, Collins R, Franzosi MG, Tognoni G, et al. 2008. Susceptibility to coronary artery disease and diabetes is encoded by distinct, tightly linked SNPs in the ANRIL locus on chromosome 9p. *Hum Mol Genet* **17:** 806–814.

Carvajal-Carmona LG, Cazier JB, Jones AM, Howarth K, Broderick P, Pittman A, Dobbins S, Tenesa A, Farrington S, Prendergast J, et al. 2011. Fine-mapping of colorectal cancer susceptibility loci at 8q23.3, 16q22.1 and 19q13.11: Refinement of association signals and use of *in silico* analysis to suggest functional variation and unexpected candidate target genes. *Hum Mol Genet* **20:** 2879–2888.

Chung CC, Ciampa J, Yeager M, Jacobs KB, Berndt SI, Hayes RB, Gonzalez-Bosquet J, Kraft P, Wacholder S, Orr N, et al. 2011. Fine mapping of a region of chromosome 11q13 reveals multiple independent loci associated with risk of prostate cancer. *Hum Mol Genet* **20:** 2869–2878.

Crabtree GR, Olson EN. 2002. NFAT signaling: Choreographing the social lives of cells. *Cell* (Suppl) **109:** S67–S79.

Crawford GE, Holt IE, Whittle J, Webb BD, Tai D, Davis S, Margulies EH, Chen Y, Bernat JA, Ginsburg D, et al. 2006. Genome-wide mapping of DNase hypersensitive sites using massively parallel signature sequencing (MPSS). *Genome Res* **16:** 123–131.

Crooks GE, Hon G, Chandonia JM, Brenner SE. 2004. WebLogo: A sequence logo generator. *Genome Res* **14:** 1188–1190.

The ENCODE Project Consortium. 2004. The ENCODE (ENCyclopedia Of DNA Elements) Project. *Science* **306:** 636–640.

The ENCODE Project Consortium. 2007. Identification and analysis of functional elements in 1% of the human genome by the ENCODE pilot project. *Nature* **447:** 799–816.

The ENCODE Project Consortium. 2011. A user's guide to the encyclopedia of DNA elements (ENCODE). *PLoS Biol* **9:** e1001046. doi: 10.1371/journal.pbio.1001046.

The ENCODE Project Consortium. 2012. An integrated encyclopedia of DNA elements in the human genome. *Nature* (in press).

Ernst J, Kheradpour P, Mikkelsen TS, Shoresh N, Ward LD, Epstein CB, Zhang X, Wang L, Issner R, Coyne M, et al. 2011. Mapping and analysis of chromatin state dynamics in nine human cell types. *Nature* **473:** 43–49.

Giresi PG, Kim J, McDaniell RM, Iyer VR, Lieb JD. 2007. FAIRE (formaldehyde-assisted isolation of regulatory elements) isolates active regulatory elements from human chromatin. *Genome Res* **17:** 877–885.

Gökçe M, Karahan B, Yilmaz R, Orem C, Erdol C, Ozdemir S. 2005. Long term effects of hormone replacement therapy on heart rate variability, QT interval, QT dispersion and frequencies of arrhythmia. *Int J Cardiol* **99:** 373–379.

Grarup N, Overvad M, Sparso T, Witte DR, Pisinger C, Jorgensen T, Yamauchi T, Hara K, Maeda S, Kadowaki T, et al. 2011. The diabetogenic *VPS13C/C2CD4A/C2CD4B* rs7172432 variant impairs glucose-stimulated insulin

response in 5,722 non-diabetic Danish individuals. *Diabetologia* **54:** 789–794.

Gross DS, Garrard WT. 1988. Nuclease hypersensitive sites in chromatin. *Annu Rev Biochem* **57:** 159–197.

Harismendy O, Notani D, Song X, Rahim NG, Tanasa B, Heintzman N, Ren B, Fu XD, Topol EJ, Rosenfeld MG, et al. 2011. 9p21 DNA variants associated with coronary artery disease impair interferon-γ signalling response. *Nature* **470:** 264–268.

Harrow J, Frankish A, Gonzalez JM, Tapanari E, Diekhans M, Kokocinski F, Aken BL, Barrell D, Zadissa A, Searle S, et al. 2012. GENCODE: The reference human genome annotation for The ENCODE Project. *Genome Res* (this issue). doi: 10.1101/gr.135350.111.

Hashiba K. 1978. Hereditary QT prolongation syndrome in Japan: Genetic analysis and pathological findings of the conducting system. *Jpn Circ J* **42:** 1133–1150.

Heit JJ, Apelqvist AA, Gu X, Winslow MM, Neilson JR, Crabtree GR, Kim SK. 2006. Calcineurin/NFAT signalling regulates pancreatic β-cell growth and function. *Nature* **443:** 345–349.

Hesselberth JR, Chen X, Zhang Z, Sabo PJ, Sandstrom R, Reynolds AP, Thurman RE, Neph S, Kuehn MS, Noble WS, et al. 2009. Global mapping of protein-DNA interactions *in vivo* by digital genomic footprinting. *Nat Methods* **6:** 283–289.

Hindorff LA, Sethupathy P, Junkins HA, Ramos EM, Mehta JP, Collins FS, Manolio TA. 2009. Potential etiologic and functional implications of genome-wide association loci for human diseases and traits. *Proc Natl Acad Sci* **106:** 9362–9367.

Hinohara K, Nakajima T, Takahashi M, Hohda S, Sasaoka T, Nakahara K, Chida K, Sawabe M, Arimura T, Sato A, et al. 2008. Replication of the association between a chromosome 9p21 polymorphism and coronary artery disease in Japanese and Korean populations. *J Hum Genet* **53:** 357–359.

Hiura Y, Fukushima Y, Yuno M, Sawamura H, Kokubo Y, Okamura T, Tomoike H, Goto Y, Nonogi H, Takahashi R, et al. 2008. Validation of the association of genetic variants on chromosome 9p21 and 1q41 with myocardial infarction in a Japanese population. *Circ J* **72:** 1213–1217.

The International HapMap Consortium. 2005. A haplotype map of the human genome. *Nature* **437:** 1299–1320.

The International HapMap Consortium. 2007. A second generation human haplotype map of over 3.1 million SNPs. *Nature* **449:** 851–861.

The International HapMap Consortium. 2010. A map of human genome variation from population-scale sequencing. *Nature* **467:** 1061–1073.

Jarinova O, Stewart AF, Roberts R, Wells G, Lau P, Naing T, Buerki C, McLean BW, Cook RC, Parker JS, et al. 2009. Functional analysis of the chromosome 9p21.3 coronary artery disease risk locus. *Arterioscler Thromb Vasc Biol* **29:** 1671–1677.

Johnson DS, Mortazavi A, Myers RM, Wold B. 2007. Genome-wide mapping of in vivo protein-DNA interactions. *Science* **316:** 1497–1502.

Kadish AH, Greenland P, Limacher MC, Frishman WH, Daugherty SA, Schwartz JB. 2004. Estrogen and progestin use and the QT interval in postmenopausal women. *Ann Noninvasive Electrocardiol* **9:** 366–374.

Kasowski M, Grubert F, Heffelfinger C, Hariharan M, Asabere A, Waszak SM, Habegger L, Rozowsky J, Shi M, Urban AE, et al. 2010. Variation in transcription factor binding among humans. *Science* **328:** 232–235.

Kent WJ, Sugnet CW, Furey TS, Roskin KM, Pringle TH, Zahler AM, Haussler D. 2002. The Human Genome Browser at UCSC. *Genome Res* **12:** 996–1006.

Kral BG, Mathias RA, Suktitipat B, Ruczinski I, Vaidya D, Yanek LR, Quyyumi AA, Patel RS, Zafari AM, Vaccarino V, et al. 2011. A common variant in the *CDKN2B* gene on chromosome 9p21 protects against coronary artery disease in Americans of African ancestry. *J Hum Genet* **56:** 224–229.

Landers JE, Melki J, Meininger V, Glass JD, van den Berg LH, van Es MA, Sapp PC, van Vught PW, McKenna-Yasek DM, Blauw HM, et al. 2009. Reduced expression of the *Kinesin-Associated Protein 3 (KIFAP3)* gene increases survival in sporadic amyotrophic lateral sclerosis. *Proc Natl Acad Sci* **106:** 9004–9009.

Lettre G, Palmer CD, Young T, Ejebe KG, Allayee H, Benjamin EJ, Bennett F, Bowden DW, Chakravarti A, Dreisbach A, et al. 2011. Genome-wide association study of coronary heart disease and its risk factors in 8,090 African Americans: The NHLBI CARe Project. *PLoS Genet* **7:** e1001300. doi: 10.1371/journal.pgen.1001300.

Locati EH, Zareba W, Moss AJ, Schwartz PJ, Vincent GM, Lehmann MH, Towbin JA, Priori SG, Napolitano C, Robinson JL, et al. 1998. Age- and sex-related differences in clinical manifestations in patients with congenital long-QT syndrome: Findings from the International LQTS Registry. *Circulation* **97:** 2237–2244.

Lou H, Yeager M, Li H, Bosquet JG, Hayes RB, Orr N, Yu K, Hutchinson A, Jacobs KB, Kraft P, et al. 2009. Fine mapping and functional analysis of a common variant in *MSMB* on chromosome 10q11.2 associated with prostate cancer susceptibility. *Proc Natl Acad Sci* **106:** 7933–7938.

Macintyre G, Bailey J, Haviv I, Kowalczyk A. 2010. is-rSNP: A novel technique for *in silico* regulatory SNP detection. *Bioinformatics* **26:** i524–i530.

Manolio TA. 2010. Genomewide association studies and assessment of the risk of disease. *N Engl J Med* **363:** 166–176.

Nakagawa M, Ooie T, Takahashi N, Taniguchi Y, Anan F, Yonemochi H, Saikawa T. 2006. Influence of menstrual cycle on QT interval dynamics. *Pacing Clin Electrophysiol* **29:** 607–613.

Ng PC, Henikoff S. 2003. SIFT: Predicting amino acid changes that affect protein function. *Nucleic Acids Res* **31:** 3812–3814.

Nicolae DL, Gamazon E, Zhang W, Duan S, Dolan ME, Cox NJ. 2010. Trait-associated SNPs are more likely to be eQTLs: Annotation to enhance discovery from GWAS. *PLoS Genet* **6:** e1000888. doi: 10.1371/journal.pgen.100088.

Paul DS, Nisbet JP, Yang TP, Meacham S, Rendon A, Hautaviita K, Tallila J, White J, Tijssen MR, Sivapalaratnam S, et al. 2011. Maps of open chromatin guide the functional follow-up of genome-wide association signals: Application to hematological traits. *PLoS Genet* **7:** e1002139. doi: 10.1371/journal.pgen.1002139.

Pique-Regi R, Degner JF, Pai AA, Gaffney DJ, Gilad Y, Pritchard JK. 2011. Accurate inference of transcription factor binding from DNA sequence and chromatin accessibility data. *Genome Res* **21:** 447–455.

Robertson G, Hirst M, Bainbridge M, Bilenky M, Zhao Y, Zeng T, Euskirchen G, Bernier B, Varhol R, Delaney A, et al. 2007. Genome-wide profiles of STAT1 DNA association using chromatin immunoprecipitation and massively parallel sequencing. *Nat Methods* **4:** 651–657.

Saccone SF, Bolze R, Thomas P, Quan J, Mehta G, Deelman E, Tischfield JA, Rice JP. 2010. SPOT: A web-based tool for using biological databases to prioritize SNPs after a genome-wide association study. *Nucleic Acids Res* **38:** W201–W209.

Samani NJ, Erdmann J, Hall AS, Hengstenberg C, Mangino M, Mayer B, Dixon RJ, Meitinger T, Braund P, Wichmann HE, et al. 2007. Genomewide association analysis of coronary artery disease. *N Engl J Med* **357:** 443–453.

Sanna S, Li B, Mulas A, Sidore C, Kang HM, Jackson AU, Piras MG, Usala G, Maninchedda G, Sassu A, et al. 2011. Fine mapping of five loci associated with low-density lipoprotein cholesterol detects variants that double the explained heritability. *PLoS Genet* **7:** e1002198. doi: 10.1371/journal.pgen.1002198.

Sayers EW, Barrett T, Benson DA, Bolton E, Bryant SH, Canese K, Chetvernin V, Church DM, Dicuccio M, Federhen S, et al. 2012. Database resources of the National Center for Biotechnology Information. *Nucleic Acids Res* **40:** D13–D25.

Schadt EE, Molony C, Chudin E, Hao K, Yang X, Lum PY, Kasarskis A, Zhang B, Wang S, Suver C, et al. 2008. Mapping the genetic architecture of gene expression in human liver. *PLoS Biol* **6:** e107. doi: 10.1371/journal.pbio.0060107.

Stranger BE, Nica AC, Forrest MS, Dimas A, Bird CP, Beazley C, Ingle CE, Dunning M, Flicek P, Koller D, et al. 2007. Population genomics of human gene expression. *Nat Genet* **39:** 1217–1224.

Sutcliffe JG, Hedlund PB, Thomas EA, Bloom FE, Hilbush BS. 2011. Peripheral reduction of β-amyloid is sufficient to reduce brain β-amyloid: Implications for Alzheimer's disease. *J Neurosci Res* **89:** 808–814.

Wei GH, Badis G, Berger MF, Kivioja T, Palin K, Enge M, Bonke M, Jolma A, Varjosalo M, Gehrke AR, et al. 2010. Genome-wide analysis of ETS-family DNA-binding *in vitro* and *in vivo*. *EMBO J* **29:** 2147–2160.

The Wellcome Trust Case Control Consortium. 2007. Genome-wide association study of 14,000 cases of seven common diseases and 3,000 shared controls. *Nature* **447:** 661–678.

Wild PS, Zeller T, Schillert A, Szymczak S, Sinning CR, Deiseroth A, Schnabel RB, Lubos E, Keller T, Eleftheriadis MS, et al. 2011. A genome-wide association study identifies LIPA as a susceptibility gene for coronary artery disease. *Circ Cardiovasc Genet* **4:** 403–412.

Xu Z, Taylor JA. 2009. SNPinfo: Integrating GWAS and candidate gene information into functional SNP selection for genetic association studies. *Nucleic Acids Res* **37:** W600–W605.

Yamauchi T, Hara K, Maeda S, Yasuda K, Takahashi A, Horikoshi M, Nakamura M, Fujita H, Grarup N, Cauchi S, et al. 2010. A genome-wide association study in the Japanese population identifies susceptibility loci for type 2 diabetes at *UBE2E2* and *C2CD4A-C2CD4B*. *Nat Genet* **42:** 864–868.

Zhong H, Beaulaurier J, Lum PY, Molony C, Yang X, Macneil DJ, Weingarth DT, Zhang B, Greenawalt D, Dobrin R, et al. 2010. Liver and adipose expression associated SNPs are enriched for association to type 2 diabetes. *PLoS Genet* **6:** e1000932. doi: 10.1371/journal.pgen.1000932.